

Polarization Properties of Nine Southern Radio PulsarsFronefield Crawford^{1,2,3}, Richard N. Manchester⁴, and Victoria M. Kaspi^{3,5,6}**ABSTRACT**

We report on radio polarimetry observations for nine southern pulsars. Six of the nine in the sample are young, with characteristic ages under 100 kyr and high spin-down luminosities. All six show a significant degree of linear polarization. We also confirm a previously noticed trend in which the degree of linear polarization increases with spin-down luminosity. Where possible we have used the rotating-vector model of the pulsar emission geometry to fit the observed position angle data. Our fit for PSR J1513–5908 (B1509–58) in particular is useful for directly testing the magnetospheric model of Melatos (1997) in combination with further timing observations. For this pulsar we find that a magnetic inclination angle greater than or equal to 60° is excluded at the 3σ level, and that the geometry suggested by the morphology of an apparent bipolar X-ray outflow is marginally inconsistent with the Melatos model. We also report on polarimetry of three older pulsars: PSR J0045–7319, PSR J1627–4845, and PSR J1316–6232 (whose discovery we also report). Of these, only PSR J0045–7319 shows significant polarization.

Subject headings: pulsars: general — ISM: magnetic fields

1. Introduction

Polarization observations of radio pulsars are a useful way to probe pulsar emission geometry, the radio emission process, and the properties of the interstellar medium (ISM). The emission

¹Lockheed Martin Management and Data Systems, P.O. Box 8048, Philadelphia, PA 19101

²Department of Physics, Haverford College, Haverford, PA 19041

³Department of Physics and Center for Space Research, Massachusetts Institute of Technology, Cambridge, MA 02139

⁴Australia Telescope National Facility, CSIRO, P.O. Box 76, Epping, NSW 1710, Australia

⁵Department of Physics, Rutherford Physics Building, McGill University, 3600 University Street, Montreal, Quebec, H3A 2T8, Canada

⁶Alfred P. Sloan Research Fellow

geometry of a pulsar can be characterized by two angles: the angle between the spin and magnetic dipole axes (the magnetic inclination angle, α), and the angle between the spin axis and the observer’s line of sight, ζ . The difference between these two angles is the impact parameter of the magnetic axis to the line of sight, β , defined according to $\beta = \zeta - \alpha$. In the rotating-vector model, the position angle (PA) of linearly polarized radiation follows the projected direction of the magnetic field axis as the pulsar rotates (Radhakrishnan & Cooke 1969). The PA, ψ , is expected to make a characteristic S-shape as the axis swings across the profile, and changes as a function of the pulse phase ϕ according to

$$\tan(\psi - \psi_0) = \frac{\sin \alpha \sin(\phi - \phi_0)}{\sin \zeta \cos \alpha - \cos \zeta \sin \alpha \cos(\phi - \phi_0)}, \quad (1)$$

where ψ_0 is the projected direction of the rotation axis of the pulsar and ϕ_0 is the phase of maximum PA swing. By rewriting the equation in terms of the directly measured β rather than ζ and fitting the observed PA values to this model, one can attempt to constrain these angles and understand the orientation of the pulsar axes (e.g., Lyne & Manchester 1988).

In addition to elucidating pulsar magnetic and spin geometries, polarization observations are useful for a variety of other reasons. For example, Melatos (1997) has proposed a model of the pulsar magnetosphere in which the pulsar and inner magnetosphere are treated as a single perfectly conducting sphere rotating in a vacuum. With three observable parameters (the period P , the period derivative \dot{P} , and α), the model predicts values for the first and second braking indices, n and m , which are defined as a function of the pulsar frequency $\nu \equiv 1/P$ and its frequency derivatives:

$$n = \frac{\nu \ddot{\nu}}{\dot{\nu}^2}, \quad (2)$$

$$m = \frac{\nu^2 \ddot{\nu}}{\dot{\nu}^3}. \quad (3)$$

The model predicts values of n for the Crab, PSR B0540–69, and PSR J1513–5908 (B1509–58) which agree with the observed values from timing data. The braking index measured for the recently discovered PSR J1119–6127 is also in good agreement with the model prediction (Camilo et al. 2000). To date, only the Crab pulsar (Lyne, Pritchard, & Graham-Smith 1993) and PSR J1513–5908 (Kaspi et al. 1994a) have had simultaneous measurements of n and m from a measured third period derivative, and PSR J1513–5908 is the only pulsar for which this has been done from absolute pulse numbering. Glitches and timing noise in the Crab pulsar may never allow a direct estimate of its m , though the Melatos (1997) prediction is consistent with current estimates obtained indirectly by Lyne, Pritchard, & Graham-Smith (1993). On the other hand, the accuracy of the spin parameters for PSR J1513–5908 should increase over time. Therefore PSR J1513–5908 is the best pulsar currently known with which to test the Melatos model. A previous estimate of $\alpha \sim 60^\circ$

was obtained for PSR J1513–5908 by fitting the pulse profiles, and the relative phase offsets of the peaks from radio, X-ray, and soft gamma-ray observations, to an outer-gap emission model (Romani & Yadigaroglu 1995). Fitting the observed polarization profile to the rotating vector model can in principle provide a more direct and reliable constraint on α .

There is a large body of literature in which the geometric interpretation of pulsar polarization phenomenology and profile forms is discussed. One interpretation (e.g., Rankin 1990, 1993a, 1993b; Gil, Kijak, & Seiradakis 1993; Rankin & Rathnasree 1997; Weisberg et al. 1999) suggests that there is a clear split between a profile component which arises from a central core beam and components which stem from one or more hollow conal beams. Another interpretation, largely due to Lyne & Manchester (1988), suggests that there is no fundamental difference in the origin of the different profile forms and that all forms arise from “patchy” beams which fill some fraction of an overall circular beam. In this scheme, a gradual change in the emission characteristics with frequency and pulse period, as well as viewing geometry, accounts for whether a pulsar is core- or cone-dominated. In this paper we retain the core and cone terminology and interpret our observed profiles in this second context, though we do not pretend to claim that we have resolved this contentious issue, which will require further extensive work.

Polarimetric observations of young radio pulsars in general indicate that they are typically more highly polarized than their older counterparts (Qiao et al. 1995; von Hoensbroech et al. 1998). Polarization profiles for some, especially young, pulsars have characteristics consistent with their emission coming from part of a possibly wide conal beam (Lyne & Manchester 1988; Manchester 1996). One consequence of this is that a significant phase offset can be observed between the profile peak, which occurs at one edge of the cone, and the point of maximum PA swing, which traces the magnetic axis. If no significant phase offset is seen, then a shallow PA swing would be present, implying a large impact parameter. Conal beams are typically more highly linearly polarized and have weak circular polarization, while core beams have weak linear polarization and a sign reversal in the circular polarization (Lyne & Manchester 1988; Rankin 1990, 1993a, 1993b). It is not known why young pulsars should exhibit strongly linearly polarized emission from conal beams and why the degree of linear polarization should increase with spin-down luminosity.

Polarization observations of pulsars also allow the determination of rotation measures (RMs) which probe the Galactic magnetic field at a variety of distances. The mean line-of-sight ISM magnetic field strength can be estimated from measurements of the RM and dispersion measure (DM) using

$$\langle B_{\parallel} \rangle = 1.232 \frac{\text{RM}}{\text{DM}} \mu\text{G}, \quad (4)$$

where RM is measured in units of rad m^{-2} and DM in units of pc cm^{-3} (Manchester & Taylor 1977). RM measurements can also help support associations between young pulsars and supernova remnants (SNRs). Traditionally this is done by measuring consistent ages and distances for the pulsar and remnant. In most cases, however, there are either significant discrepancies or large

uncertainties in these estimates. If the RM of the pulsar and the RM of the SNR at the location of the pulsar are consistent with each other, then an association would be supported.

We report on radio polarization observations for six young southern radio pulsars. These pulsars all have characteristic ages $\tau_c \equiv P/2\dot{P} < 100$ kyr and spin-down luminosities $\dot{E} \equiv 4\pi^2 I \dot{P}/P^3 > 10^{34}$ erg s⁻¹, where I is an assumed moment of inertia of 10^{45} g cm². Polarization results for most of the rest of the young pulsar population can be found elsewhere (e.g., Qiao et al. 1995; Gould & Lyne 1998; Manchester, Han, & Qiao 1998; von Hoensbroech et al. 1998; Weisberg et al. 1999 and references therein). We also report on polarimetry of three pulsars which are not particularly young, but are interesting for other reasons: PSR J0045–7319 is in a binary orbit with a B-star companion, PSR J1316–6232, whose discovery we also report, is spatially coincident with a region of extended radio emission, and PSR J1627–4845 is spatially coincident with SNR G335.2+0.1. The properties for the pulsars in our sample are listed in Table 1.

2. Observations and Data Reduction

All pulsars in our sample were observed with the Parkes 64-m radio telescope in NSW, Australia, from 17 - 24 February 1997 at 1350 MHz, except PSR J0045–7319 which was observed at 660 MHz. Follow-up observations were conducted on several pulsars on 15 - 16 January 1998 at 660 and 2260 MHz. Table 2 lists the parameters for the observations. The details of the hardware setup and observing technique are the same as those reported elsewhere (Navarro 1994; Navarro et al. 1997; Manchester, Han, & Qiao 1998). Observations were made in pairs at orthogonal feed angles and summed to minimize the effects of instrumental polarization. Residual instrumentation effects contributed at most a few percent of the total intensity to the measured Stokes parameters.

In cases where we did not have an initial RM estimate, an improper RM correction to the data could cause the PAs from different frequency channels to wind by more than one rotation and add destructively. Therefore, we tried a large range of RMs, typically ± 100 DM rad m⁻², where DM is in units of pc cm⁻³. In most cases, one of the trial RMs yielded a significantly larger linear polarization magnitude than the others. We used this RM as the starting point for our RM convergence.

3. Results and Discussion

Seven of the nine pulsars (including all six of the young pulsars) show linear polarization which is significant enough to permit an RM estimate. The measured polarization parameters for the pulsars are listed in Table 3, with L and V representing linearly and circularly polarized intensity respectively. The polarization profiles for the seven pulsars for which there was significant polarization appear in Figure 1. All of the profiles in this figure are at 1350 MHz, except for PSR J0045–7319 and the additional profile for PSR J1513–5908, both of which are at 660 MHz. Position

angles with more than 20° uncertainty were not plotted except in the case of PSR J0045–7319 which was weak and therefore had an imposed cutoff of 40° uncertainty. Table 4 lists the RMs and mean line-of-sight magnetic field strength estimates with 1σ uncertainties for each. Total intensity pulse widths are also included in Table 4. In several cases the PA could be measured over a significant fraction of the 1350 MHz profile with good signal-to-noise. For these pulsars we attempted to fit the observed PA swing over the profile to the rotating-vector model.

Below we outline the polarization results for each pulsar separately.

3.1. PSR J0045–7319

PSR J0045–7319 was the first pulsar discovered in the Small Magellanic Cloud (SMC) (McConnell et al. 1991) and is in a 51-day binary orbit around a B1 class V star (Kaspi et al. 1994b). The wind from the B star, however, is very tenuous and has been shown to contribute little to the DM (Kaspi et al. 1996a). This is consistent with our results which indicate that during periastron passage (from 18 February 1997 to 23 February 1997) the RM remains small.

The 660 MHz polarization profile, compiled from a total of about 8 hours of observations made over 6 days, shows slight linear and more significant circular polarization with large uncertainties in each. The pulsar flux and polarization, however, are too weak to allow us to say anything meaningful about the PA swing and emission geometry. However, a secondary component to the right of the main peak is likely one of the outlying profile components which is clearly visible in higher frequency profiles. Since the majority of the contribution to the DM ($\sim 75\%$) is likely to be from the SMC itself, the measured RM (and mean line-of-sight magnetic field strength) is strongly weighted toward the ISM of the SMC. The very low value of $-0.2 \pm 0.3 \mu\text{G}$ for $\langle B_{\parallel} \rangle$ indicates that this part of the SMC has magnetic fields which are either tangled or largely perpendicular to the line of sight.

3.2. PSR J1105–6107

PSR J1105–6107 is a young and energetic pulsar: its $\dot{E} = 2.5 \times 10^{36} \text{ erg s}^{-1}$, and its characteristic age is 63 kyr (Kaspi et al. 1997). As Figure 1 shows, the 1350 MHz polarization profile shows two peaks separated by $\sim 40^\circ$. The profile is $\sim 100\%$ and $\sim 80\%$ linearly polarized over the first and second peaks respectively. The second peak shows a slight increase in left-handed circular polarization, though it remains weak. The high degree of linear polarization and offset of the PA swing from the pulse peak suggest that the emission is from the leading edge of a cone. The occurrence of the maximum PA swing after the double peak indicates that both components are likely part of the leading edge of the conal beam (Lyne & Manchester 1988; Manchester 1996). Our attempt to fit the PA data from PSR J1105–6107 to the rotating-vector model did not yield a reliable result and no formal constraints on the geometry of the pulsar can be given.

3.3. PSR J1316–6232

PSR J1316–6232 is a 343-ms pulsar with a large DM (983 pc cm^{-3}) that was serendipitously discovered in the same survey targeting OB stars in which PSR J1105–6107 was discovered (Kaspi et al. 1997). However, neither pulsar is associated with a target OB star; we report the discovery of PSR J1316–6232 here. Since its discovery, timing observations have been carried out at the Parkes Observatory using a hardware setup and analysis procedure which is described elsewhere (D’Amico et al. 1998). A total of 90 observations spanning 733 days were used at frequencies ranging from 1390 to 2000 MHz. Arrival times for the observations were fitted using the TEMPO software package⁷, with an rms timing residual of ~ 5 ms. The best-fit timing parameters for the pulsar are given in Table 5.

The profile at 1350 MHz has a large asymmetric tail due to multipath ISM scattering with a time constant $\tau_s \sim 150$ ms. Scattering may be smearing any linearly polarized emission, but at 2260 MHz, the scattering is significantly reduced and still no significant linearly polarized emission is seen. The scattering at 2260 MHz is expected to be $\lesssim 20$ ms, but the profile still has a scattered appearance with $\tau_s \sim 50$ ms. It is likely that there is an intrinsic component to the tail. The pulse width remains large at high frequencies, with a duty cycle of $\sim 20\%$. No individual components can be resolved in the profile. A 4.85 GHz map of the region from the Parkes-MIT-NRAO Southern Survey (Condon, Griffith, & Wright 1993) shows a region of extended radio emission coincident with the position of the pulsar. This may account for the large DM and scattering if this region is in front of the pulsar. However, it is unlikely that this would cause significant Faraday smearing since the RM magnitudes that would be necessary ($\text{RM} > 10^4 \text{ rad m}^{-2}$) far exceed observed Galactic RM values (Gray et al. 1999). It is more likely that PSR J1316–6232 is simply intrinsically unpolarized.

3.4. PSR J1341–6220 (B1338–62)

PSR J1341–6220 (B1338–62) is a young pulsar with $P = 193$ ms and an age of 12 kyr (Kaspi et al. 1992). As shown in Figure 1, at 1350 MHz the pulsar shows significant linear polarization (56%) and right-handed circular polarization (21%). A previous estimate of the linear polarization at 1400 MHz by Qiao et al. (1995) was somewhat higher (80%) but had a significantly larger uncertainty ($\sim 10\%$) than the results quoted here. A scattering tail of length ~ 8 ms is evident, which is not surprising considering the high DM (730 pc cm^{-3}), and this has affected the polarization properties, particularly in the trailing part of the pulse. Because of this we did not attempt to fit the rotating-vector model to the PA data.

⁷<http://pulsar.princeton.edu/tempo>

3.5. PSR J1513–5908 (B1509–58)

PSR J1513–5908 (B1509–58) was first discovered as an X-ray source (Seward & Harnden 1982) and was subsequently found to be a radio pulsar (Manchester, Tuohy, & D’Amico 1982). Timing observations showed that it has a large $\dot{E} = 2 \times 10^{37}$ erg s⁻¹ and a small characteristic age ($\tau_c \sim 1.5$ kyr). The pulsar is located near SNR G320.4–1.2; the two are almost certainly associated (Gaensler et al. 1999).

Profiles for PSR J1513–5908 at both 660 and 1350 MHz are shown in Figure 1. At 660 MHz the profile is broad and probably affected by interstellar scattering. There is good evidence at 1350 MHz for a weak component preceding the main pulse by $\sim 50^\circ$ of longitude. At both frequencies the emission is almost completely linearly polarized, with significant right-handed circular polarization as well. The high degree of linear polarization, shallow PA swing, and absence of a sign change in the circular polarization over the profile all support the notion that the emission is from the grazing edge of a conal beam component.

There is no significant falloff in the degree of linear polarization between 660 and 1350 MHz; if a falloff occurs, it is at higher frequencies (Manchester et al. 1973; Manchester & Taylor 1977). The unchanging linear polarization supports the observation of von Hoensbroech et al. (1998) that high- \dot{E} pulsars do not suffer as significantly from depolarization effects at high frequencies as do low- \dot{E} pulsars.

The RM estimates from the data at the two frequencies ($+211 \pm 5$ rad m⁻² for 660 MHz and $+215 \pm 2$ rad m⁻² for 1350 MHz) are consistent with each other and are consistent with the RM of SNR G320.4–1.2 of $+210 \pm 30$ rad m⁻² at the location of the pulsar (Gaensler et al. 1999). This supports the association between the pulsar and the remnant, considering that the RM in different parts of the SNR can vary by hundreds of rad m⁻².

As mentioned in §1, the magnetospheric model of Melatos (1997) can be tested with an accurate determination of the emission geometry of PSR J1513–5908. In particular, an estimate of α can be used along with P and \dot{P} to make predictions for the braking indices n and m . These predictions can be compared to the measured values of n and m from pulsar timing (Kaspi et al. 1994a). From our fit of the 1350 MHz data to the rotating-vector model, values of $\alpha \geq 60^\circ$ are excluded at the 3σ level. An estimate of $\sim 60^\circ$ was suggested from a fit of the high-energy pulse profile to an outer-gap model (Romani & Yadigaroglu 1995). Our result suggests that this value is unlikely.

For an inclination angle range of $\alpha < 60^\circ$, the Melatos (1997) model predicts that the first braking index should be $n < 2.92$ for PSR J1513–5908. The observed value of 2.837 ± 0.001 (Kaspi et al. 1994a) falls easily in this range. For $\alpha < 60^\circ$, the second braking index is predicted by the model to be $m < 14.0$. Currently the best measured value for this parameter is $m = 14.5 \pm 3.6$ (Kaspi et al. 1994a), which partially overlaps the predicted range. Therefore the Melatos model cannot be directly tested using current data, but this should be possible in the future.

The swing of the observed PA data is shallow, implying a large impact parameter. However,

fitted values of α and ζ are highly covariant because of the limited longitude extent of the observed pulse profile; for $\alpha = 60^\circ$, $\zeta = 130^\circ$ and for $\alpha = 45^\circ$, $\zeta = 100^\circ$. Therefore the observations are consistent with the estimate of $\zeta \gtrsim 70^\circ$ from Brazier & Becker (1997), obtained by interpreting the X-ray morphology of the surrounding region as the result of a bipolar outflow from the pulsar with an equatorial torus. However, by imposing the restriction that $\zeta > 70^\circ$ in our fit, we find that $\alpha > 30^\circ$ at the 3σ level, which corresponds to a prediction of $n > 2.86$ in the Melatos model. This is marginally inconsistent with the observed value of $n = 2.837 \pm 0.001$ (Kaspi et al. 1994a).

3.6. PSR J1627–4845

PSR J1627–4845 was one of two new pulsars discovered in a targeted search of southern supernova remnants (Kaspi et al. 1996b) and is spatially coincident with SNR G335.2+0.1. However, the discrepancy in the ages of the objects argues that the spatial association is only a chance superposition. We were unable to detect significant linear polarization or determine a rotation measure for this pulsar at 1350 MHz. It is likely that the intrinsic polarization is low as might be expected for an old pulsar.

3.7. PSR J1646–4346 (B1643–43)

PSR J1646–4346 (B1643–43) is a 232-ms pulsar with a characteristic age of 32 kyr (Johnston et al. 1995). As Figure 1 shows, our polarization profile is noisy but has significant linear polarization (45%) and negligible circular polarization. There is also a slight profile asymmetry probably from multipath scattering ($\tau_s \sim 11$ ms). The estimated RM of -65 ± 17 rad m⁻² implies $\langle B_{\parallel} \rangle = -0.16 \pm 0.04$ μ G, which is consistent with Galactic magnetic field strengths.

3.8. PSR J1730–3350 (B1727–33)

PSR J1730–3350 (B1727–33) has a period of 139 ms and is young, with a characteristic age of 26 kyr (Johnston et al. 1995). The polarization profile at 1350 MHz shown in Figure 1 shows significant linear polarization (56%) with weak circular polarization. This is consistent with the results of Gould & Lyne (1998) who find the degree of linear polarization to be 48% at 1400 MHz. There is also a significant scattering tail ($\tau_s \sim 7$ ms) from multipath scattering, and the linear polarization in the trailing part of the profile is affected by this. The rapid PA swing in the leading part of the profile indicates a small impact parameter. The intrinsic profile probably has a somewhat higher polarization with a rapid PA swing over a greater range than that observed. A fit to the PA data preceding the profile peak (where scattering has little effect) indicates that $|\beta| < 5^\circ$ at the 3σ confidence level. The measured RM of -142 ± 5 rad m⁻² implies $\langle B_{\parallel} \rangle = -0.68 \pm 0.02$ μ G. This RM is consistent with RM measurements of other pulsars in the region with comparable

DMs.

3.9. PSR J1801–2306 (B1758–23)

PSR J1801–2306 (B1758–23) was discovered in a search for pulsars directed at Galactic objects (Manchester, D’Amico, & Tuohy 1985). This pulsar was found to be near SNR W28, which led to speculation that the pulsar and remnant were associated (Manchester et al. 1991). The pulsar’s characteristic age of 58 kyr is consistent with the estimated age of W28 of between 35 and 150 kyr (Kaspi et al. 1993), but there is a discrepancy between the remnant distance of ~ 3 kpc (Frail, Kulkarni, & Vasisht 1993) and the pulsar distance, which is estimated from its DM to be ~ 13 kpc (Taylor & Cordes 1993). Attempts have been made to resolve this discrepancy by introducing an HII region in the line of sight which could contribute to the bulk of the dispersion (Frail, Kulkarni, & Vasisht 1993). However, there is no clear evidence for such an HII region (Kaspi et al. 1993).

The pulse profile at 1350 MHz shows a smaller degree of linear polarization (14%) than the other young pulsars we have observed, and is consistent with the estimate of Gould & Lyne (1998), who find that the linear polarization is 15% at both 1400 and 1600 MHz. The relatively small degree of polarization could be due to depolarization from profile smearing from the strong scattering ($\tau_s \sim 100$ ms) and from differential Faraday rotation along the different scattering paths in a region of high magnetic field and electron density (such as an HII region or SNR). At 2260 MHz we find that the linear polarization is low, less than a few percent, despite the significant decrease in the scattering ($\tau_s \sim 15$ ms). The RM can be estimated from the 1350 MHz data and is large and negative (Table 4). We conclude that PSR J1801–2306 is intrinsically less polarized than the other young pulsars in our sample. This is consistent with the trend noted in Figure 2 since PSR J1801–2306 has a smaller \dot{E} than these pulsars (see below).

3.10. Linear Polarization vs. Spin-down Luminosity

By comparing the measured degree of linear polarization of our young pulsars with their spin-down luminosities, \dot{E} , we confirm a trend previously noticed by several authors (Wu et al. 1993; Qiao et al. 1995; von Hoensbroech et al. 1998) in which linear polarization increases with spin-down luminosity. Figure 2 shows measured linear polarization as a function of spin-down luminosity for our six young pulsars at 1350 MHz (open circles) and for 278 pulsars from Gould and Lyne (1998) at 1400 MHz (dots). Our young pulsars are concentrated at the high- \dot{E} end of the plot while the Gould and Lyne pulsars span an \dot{E} range from 10^{30} to 10^{37} erg s $^{-1}$. The figure shows a trend in which pulsars with $\dot{E} > 10^{34}$ erg s $^{-1}$ tend to have stronger linear polarization as \dot{E} increases. The six young pulsars in our sample show this trend clearly.

von Hoensbroech et al. (1998) noticed a stronger correlation in a sample of 32 pulsars at a much higher frequency (4.9 GHz). Their trend extends down to about 10^{32} erg s $^{-1}$. Gould & Lyne

(1998) find no such correlation at 400 MHz for any \dot{E} range, and von Hoensbroech et al. conclude that depolarization effects at high frequencies affect low- \dot{E} pulsars much more strongly than they do high- \dot{E} ones. Our 1350 MHz results confirm these trends.

4. Conclusions

We have reported on radio polarimetry observations of nine southern radio pulsars. Significant polarization was detected in seven of the nine, including all six of the young pulsars in the sample. The two pulsars with no detectable polarization (PSRs J1316–6232 and J1627–4845) are older, with characteristic ages $\tau_c > 1$ Myr. With the exception of PSR J1801–2306, all of our young pulsars exhibit a high degree of linear polarization and a low degree of circular polarization. This is consistent with the suggestion of Manchester (1996) that young pulsars exhibit partial conal emission. The rotating-vector model fit of the PSR J1513–5908 data indicates that a magnetic inclination angle of $\alpha \geq 60^\circ$ is excluded at the 3σ confidence level. This result suggests that the value of $\alpha \sim 60^\circ$ estimated for this pulsar by Romani & Yadigaroglu (1995) is possible but unlikely. Imposing the restriction in the fit that $\zeta > 70^\circ$ from Brazier & Becker (1997) implies that $\alpha > 30^\circ$ at the 3σ level. For $\alpha > 30^\circ$, the predicted braking index $n > 2.86$ from the Melatos (1997) model is marginally inconsistent with the observed value of $n = 2.837 \pm 0.001$ (Kaspi et al. 1994a). Thus the predictions of the Melatos model and the limit of $\zeta \gtrsim 70^\circ$ derived by Brazier & Becker (1997) are marginally inconsistent with each other. Finally, we confirm at 1350 MHz a positive correlation between degree of linear polarization and spin-down luminosity.

We thank N. D’Amico for his assistance in the search that found PSR J1316–6232, and M. Bailes and R. Pace for help with the subsequent timing. FC thanks D. Fox for helpful discussions regarding model fitting. The Parkes radio telescope is part of the Australia Telescope, which is funded by the Commonwealth of Australia for operation as a National Facility operated by CSIRO. VMK was supported in part by an Alfred P. Sloan Research Fellowship, NSF Career Award (AST-9875897), and NSERC grant RGPIN 228738-00.

REFERENCES

- Brazier, K. T. S. & Becker, W. 1997, MNRAS, 284, 335
- Camilo, F., Kaspi, V. M., Lyne, A. G., Manchester, R. N., Bell, J. F., D’Amico, N., McKay, N. P. F., & Crawford, F. 2000, ApJ, 541, 367
- Condon, J. J., Griffith, M. R., & Wright, A. E. 1993, AJ, 106, 1095
- D’Amico, N., Stappers, B. W., Bailes, M., Martin, C. E., Bell, J. F., Lyne, A. G., & Manchester, R. N. 1998, MNRAS, 297, 28

- Frail, D. A., Kulkarni, S. R., & Vasisht, G. 1993, *Nature*, 365, 136
- Gaensler, B. M., Brazier, K. T. S., Manchester, R. N., Johnston, S., & Green, A. J. 1999, *MNRAS*, 305, 724.
- Gil, J. A., Kijak, J., & Seiradakis, J. H. 1993, *A&A*, 272, 268
- Gould, D. M. & Lyne, A. G. 1998, *MNRAS*, 301, 235
- Gray, A. D., Landecker, T. L., Dewdney, P. E., Taylor, A. R., Willis, A. G., & Normandeau, M. 1999, *ApJ*, 514, 221
- Johnston, S., Manchester, R. N., Lyne, A. G., Kaspi, V. M., & D’Amico, N. 1995, *A&A*, 293, 795
- Kaspi, V. M., Manchester, R. N., Johnston, S., Lyne, A. G., & D’Amico, N. 1992, *ApJ*, 399, L155
- Kaspi, V. M., Lyne, A. G., Manchester, R. N., Johnston, S., D’Amico, N., & Shemar, S. L. 1993, *ApJ*, 409, L57
- Kaspi, V. M., Manchester, R. N., Siegman, B., Johnston, S., & Lyne, A. G. 1994a, *ApJ*, 409, L57
- Kaspi, V. M., Johnston, S., Bell, J. F., Manchester, R. N., Bailes, M., Bessell, M., Lyne, A. G., D’Amico, N. 1994b, *ApJ*, 423, L43
- Kaspi, V. M., Tauris, T. M., & Manchester, R. N. 1996a, *ApJ*, 459, 717
- Kaspi, V. M., Manchester, R. N., Johnston, S., Lyne, A. G., & D’Amico, N. 1996b, *AJ*, 111, 2028
- Kaspi, V. M., Bailes, M., Manchester, R. N., Stappers, B. W., Sandhu, J. S., Navarro, J., & D’Amico, N. 1997, *ApJ*, 485, 820
- Lyne, A. G. & Manchester, R. N. 1988, *MNRAS*, 234, 477
- Lyne, A. G., Pritchard, R. S., & Graham-Smith, F. 1993, *MNRAS*, 265, 1003
- Manchester, R. N. & Taylor J. H. 1977, *Pulsars*, San Francisco: Freeman
- Manchester, R. N., Tademaru, E., Taylor, J. H., & Huguenin, G. R. 1973, *ApJ*, 185, 951
- Manchester, R. N., Tuohy, I. R., & D’Amico, N. 1982, *ApJ*, 262, L31
- Manchester, R. N., D’Amico, N., & Tuohy, I. R. 1985, *MNRAS*, 212, 975
- Manchester, R. N., Kaspi, V. M., Johnston, S., Lyne, A. G., & D’Amico, N. 1991, *MNRAS*, 253, 7P
- Manchester, R. N. 1996, in *IAU Colloq. 160, Pulsars: Problems and Progress*, ed. S. Johnston, M. Bailes, & M. Walker (ASP Conf. Ser. 105; San Francisco: ASP), 193

- Manchester, R. N., Han, J. L., & Qiao, G. J. 1998, *MNRAS*, 295, 280
- McConnell, D., McCulloch, P. M., Hamilton, P. A., Ables, J. G., Hall, P. J., Jacka, C. E., & Hunt, A. J. 1991, *MNRAS*, 249, 654
- Melatos, A. 1997, *MNRAS*, 288, 1049
- Navarro, J. 1994, PhD thesis, California Institute of Technology
- Navarro, J., Manchester, R. N., Sandhu, J. S., Kulkarni, S. R., & Bailes, M. 1997, *ApJ*, 486, 1019
- Qiao, G. J., Manchester, R. N., Lyne, A. G., & Gould D. M. 1995, *MNRAS*, 274, 572
- Radhakrishnan, V. & Cooke, D. J. 1969, *Astrophys. Lett.*, 3, 225
- Rankin, J. M. 1990, *ApJ*, 352, 247
- Rankin, J. M. 1993a, *ApJ*, 405, 285
- Rankin, J. M. 1993b, *ApJS*, 85, 145
- Rankin, J. M. & Rathnasree, N. 1997, *Journal of Astrophysics and Astronomy*, 18, 91
- Romani, R. W. & Yadigaroglu, I.-A. 1995, *ApJ*, 438, 314
- Seward, F. D. & Harnden, F. R., Jr. 1982, *ApJ*, 256, L45
- Taylor, J. H. & Cordes, J. M. 1993, *ApJ*, 411, 674
- von Hoensbroech, A., Kijak, J., & Krawczyk, A. 1998, *A&A*, 334, 571
- Weisberg, J. M. et al. 1999, *ApJS*, 121, 171
- Wu, X., Manchester, R. N., Lyne, A. G., & Qiao, G. 1993, *MNRAS*, 261, 630

Table 1. Pulsar Characteristics

PSR	P (sec)	DM (pc cm ⁻³)	log τ_c ^a (yr)	log B ^b (G)	log \dot{E} ^c (erg s ⁻¹)
J0045–7319	0.926	105	6.5	12.3	32.3
J1105–6107	0.063	271	4.8	12.0	36.4
J1316–6232	0.343	983	6.0	12.2	33.7
J1341–6220	0.193	730	4.1	12.9	36.2
J1513–5908	0.151	255	3.2	13.2	37.3
J1627–4845	0.612	557	6.4	12.2	32.8
J1646–4346	0.232	490	4.5	12.7	35.6
J1730–3350	0.139	257	4.4	12.5	36.1
J1801–2306	0.415	1074	4.8	12.8	34.8

^aCharacteristic age $\tau_c \equiv P/2\dot{P}$.

^bSurface dipole magnetic field strength $B \equiv 3.2 \times 10^{19} (P\dot{P})^{1/2}$ G.

^cSpin-down luminosity $\dot{E} \equiv 4\pi^2 I \dot{P} / P^3$.

Table 2. Observing Parameters

PSR	Date	Freq (MHz)	T_{int} ^a (min)	N_{bins} ^b	BW ^c (MHz)	N_{chan} ^d
J0045–7319	Feb 1997	660	464	256	32	8
J1105–6107	Feb 1997	1350	66	512	128	16
J1316–6232	Feb 1997	1350	72	128	128	64
	Jan 1998	2264	177	256	128	8
J1341–6220	Feb 1997	1350	24	512	128	32
J1513–5908	Jan 1998	660	372	128	32	8
	Feb 1997	1350	192	256	128	32
J1627–4845	Feb 1997	1350	24	512	128	32
J1646–4346	Feb 1997	1350	27	512	128	32
J1730–3350	Feb 1997	1350	30	512	128	16
J1801–2306	Feb 1997	1350	129	128	128	64
	Jan 1998	2264	372	256	128	8

^aTotal integration time.

^bNumber of bins in profile.

^cObserving bandwidth.

^dNumber of frequency channels.

Table 3. Pulsar Polarization Parameters

PSR	Freq (MHz)	S ^a (mJy)	$\langle L \rangle / S$ ^b (%)	$\langle V \rangle / S$ ^c (%)	$\langle V \rangle / S$ ^d (%)	error ^e (%)
J0045–7319	660	0.7	11	–17	27	7
J1105–6107	1350	1.0	89	+9	12	2
J1316–6232	1350	1.8	–	–	–	–
	2264	0.6	–	–	–	–
J1341–6220	1350	2.3	56	–21	22	2
J1513–5908	660	2.6	97	–23	25	7
	1350	1.3	94	–18	18	2
J1627–4845	1350	0.5	–	–	–	–
J1646–4346	1350	0.8	45	+6	13	5
J1730–3350	1350	3.3	56	–5	7	1
J1801–2306	1350	6.2	14	+12	13	2
	2264	2.1	–2	+7	12	4

^aMean flux density.

^bFractional linear polarization of on-pulse bins.

^cFractional circular polarization of on-pulse bins. Positive values are left-circularly polarized.

^dFractional value of absolute circular polarization of on-pulse bins.

^e 2σ uncertainty in polarization values. The uncertainty due to instrumental effects is at most a few percent.

Table 4. Measured Pulse Widths and Rotation Measures

PSR	Freq (MHz)	W_{50} ^a (ms)	W_{10} ^b (ms)	RM (rad m ⁻²)	$\langle B_{\parallel} \rangle$ ^c (μ G)
J0045–7319	660	20	220	-14 ± 27	-0.2 ± 0.3
J1105–6107	1350	4	10	$+166 \pm 3$	$+0.76 \pm 0.01$
J1316–6232	1350	119	180	–	–
	2264	81	115	–	–
J1341–6220	1350	10	45	-946 ± 7	-1.60 ± 0.01
J1513–5908	660	36	75	$+211 \pm 5$	$+1.02 \pm 0.03$
	1350	14	40	$+215 \pm 2$	$+1.046 \pm 0.008$
J1627–4845	1350	32	170	–	–
J1646–4346	1350	12	70	-65 ± 17	-0.16 ± 0.04
J1730–3350	1350	7	20	-142 ± 5	-0.68 ± 0.02
J1801–2306	1350	88	265	-1156 ± 19	-1.33 ± 0.02
	2264	19	80	–	–

^aWidth at which the measured pulse reaches 50% of its peak (FWHM), with uncertainty 1 ms.

^bWidth at which the measured pulse reaches 10% of its peak, with uncertainty 5 ms.

^cNegative values correspond to the magnetic field pointing away from observer.

Table 5. Astrometric and Spin Parameters for PSR J1316–6232

Parameter	Value ^a
Right Ascension, α (J2000)	13 ^h 16 ^m 46 ^s .3(2)
Declination, δ (J2000)	–62°32′12″.2(5)
Galactic Latitude, l	305°.85
Galactic Longitude, b	+0°.19
Period, P	0.34282539844(6) s
Period Derivative, \dot{P}	5.297(2) $\times 10^{-15}$
Dispersion Measure, DM	983(2) pc cm ⁻³
Epoch of Period	MJD 49800.0000
Timing Span	MJD 49729 to MJD 50462
Timing Residual	4.67 ms

^aUncertainties in parentheses apply to the last digit.

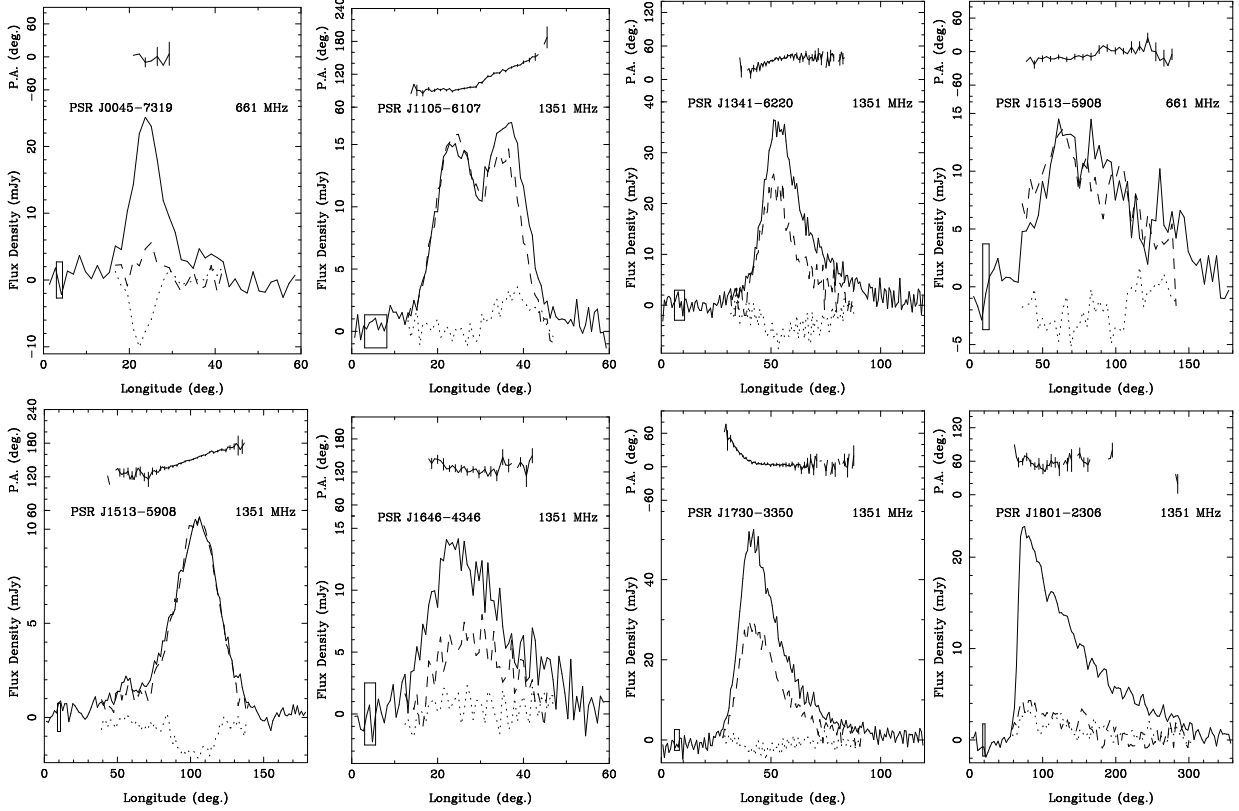


Fig. 1.— Polarization profiles for pulsars showing significant polarization. In the lower half of each plot, the solid line indicates total intensity as a function of pulse phase in degrees. The total intensity has been normalized to S , the mean flux density, using observations of Hydra A. The dashed and dotted lines indicate linearly and circularly polarized intensity respectively. Positive values of circular polarization are left-circularly polarized. The height of the box in the lower left-hand corner is twice the root-mean-square (rms) scatter, σ , in the profile baseline. The upper half of each plot shows the position angle as a function of pulse phase. The pulsar name and center frequency of the observation are also indicated in each plot.

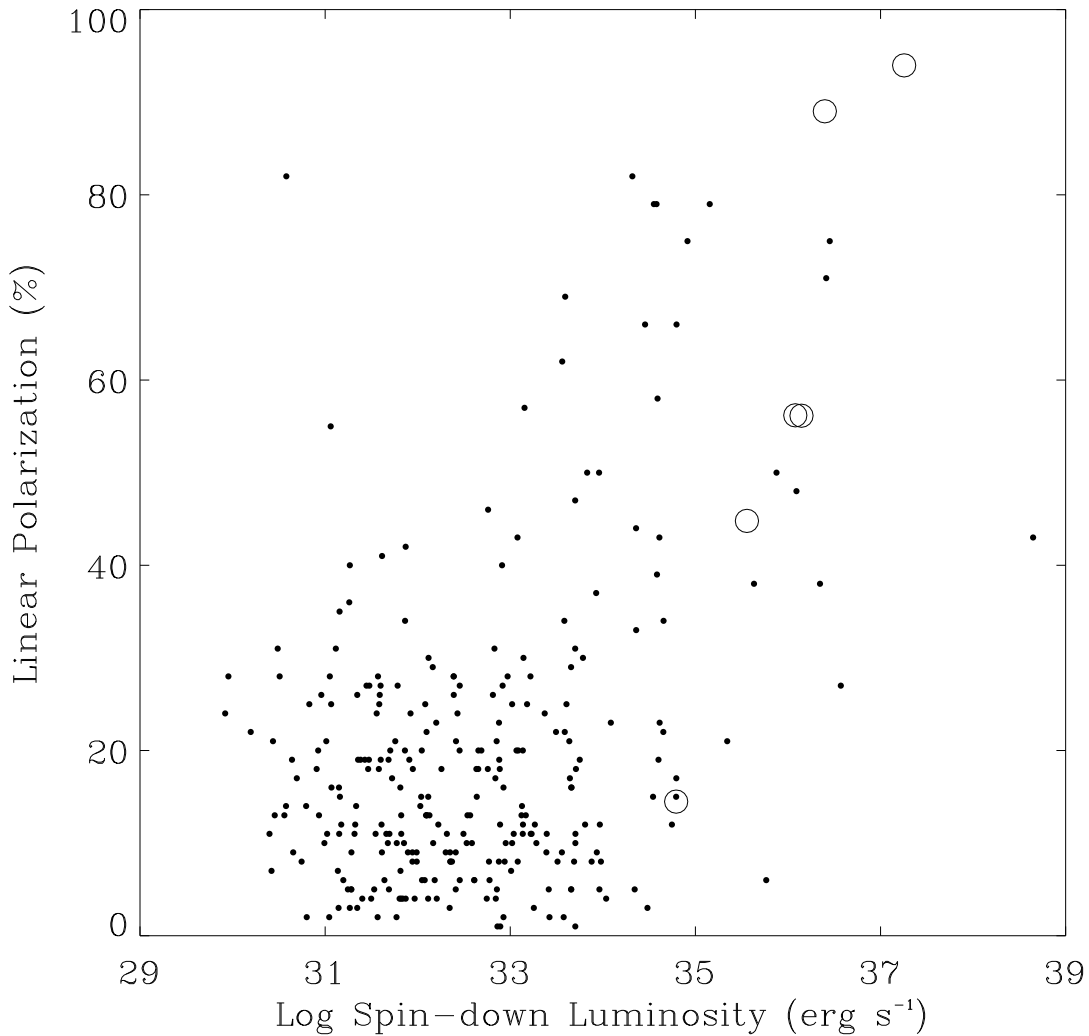


Fig. 2.— Linear polarization as a function of $\log \dot{E}$ for the six young pulsars in our sample at 1350 MHz (open circles) and 278 pulsars from the 1400 MHz data of Gould & Lyne (1998) (dots). There is a clear trend toward stronger linear polarization at high \dot{E} in both samples.